Faceting in Bond-Oriented Glasses and Quasicrystals

T. L. Ho, J. A. Jaszczak, Y. H. Li, and W. F. Saam

Department of Physics, The Ohio State University, Columbus, Ohio 43210
(Received 1 April 1987)

We show that long-range positional order in the sense that the density Fourier transform is a set of δ functions is not essential for the phenomenon of facet formation. Facets can occur in certain classes of perfect bond-oriented systems which lack the conventional long-range positional order, allowing the appearance of widths in the diffraction peaks. The predicted facets in some of these systems are consistent with the recently observed triacontahedral grain shapes in Al_6LiCu_3 and dodecahedral grain shapes in Al-Mn-Si, as well as strong spatial disorder as indicated by the x-ray diffraction measurements.

PACS numbers: 61.50.Cj, 61.40.+b

It is well known that both in equilibrium[1] and during growth processes,[2] crystal surfaces often have facets. The phenomenon of facet formation is generally thought to be a consequence of the long-range positional order (LRPO) of the system. This conventional wisdom is called into question by the icosahedral phase recently discovered[3,4] in Al_6LiCu_3. This icosahedral phase has two important features. Its grains have facets, and its x-ray diffraction peaks[5] show radial widths very similar to those in Al-Mn, reflecting a short-range positional order with a correlation length of 10^2–10^3 Å. The fascinating aspect of these features is that they appear to be inconsistent with each other. While it is generally believed that LRPO is the origin of facets, the x-ray measurements show that this seemingly crucial element is absent.

The observed grain shape[3,4] in Al_6LiCu_3 is a rhombic triacontahedron, and Al-Mn-Si exhibits dodecahedral grain shapes.[6] In general, the largest growth facets at $T \neq 0$ will also be the largest equilibrium facets at $T = 0$.[2,7] The $T \neq 0$ growth shape thus provides useful information about the $T = 0$ equilibrium shape (which reflects directly the directions of the dominant bonds in the system), and vice versa.

In this Letter, we present the simplest possible $T = 0$ equilibrium shapes for perfect bond-oriented systems (PBOS's) with icosahedral symmetry, a sufficient condition for faceting which has no apparent relation to LRPO, and an example ("quasiglass") demonstrating that a positionally disordered system can have facets.

The PBOS's considered here all have the following property: The pair correlation function $v(\mathbf{r},\mathbf{A}) \equiv \rho(\mathbf{r}) \times \rho(\mathbf{r}+\mathbf{A})$ *within the range of interaction A^* between atoms,* is of the form

$$v(\mathbf{r},\mathbf{A}) = \sum_\tau \delta(\mathbf{A}-\mathbf{A}_\tau)h(\mathbf{r},\mathbf{A}_\tau), \quad A < A^*, \tag{1}$$

where $\rho(\mathbf{r})$ is the density, and $\mathbf{A}_\tau$ is a finite set of specified vectors whose appearance is determined by the function h. According to Eq. (1), each atom in the system has neighbors in only a finite set of directions. A PBOS may or may not have LRPO. The existence of LRPO implies that the diffraction pattern consists of a set of δ-function Bragg peaks. If the peaks have widths

Δk, the positional order is no longer long range, but has a correlation length $\simeq \pi/\Delta k$. Independent of the existence of LRPO, the bulk average of the correlation function,

$$v(\mathbf{A}) \equiv \langle v(\mathbf{r},\mathbf{A})\rangle_\Omega = \int_\Omega dV\, v(\mathbf{r},\mathbf{A})\Big/\int_\Omega dV,$$

over a large volume Ω is a finite set of δ functions, $v(\mathbf{A}) = \sum_\tau \delta(\mathbf{A}-\mathbf{A}_\tau)h(\mathbf{A}_\tau)$, where $h(\mathbf{A}_\tau) \equiv \langle h(\mathbf{r},\mathbf{A}_\tau)\rangle_\Omega$, and $A < A^*$. PBOS's without LRPO are referred to as bond-oriented glasses. Although the observed icosahedral phases may not be PBOS's, Eq. (1) is satisfied by all currently proposed models for the icosahedral phase. Our motivation for studying these systems, however, is to demonstrate that bond-oriented glasses have facets.

(1) *A sufficient condition for faceting in PBOS's and the "simple bond-oriented glass."*—Let us recall that equilibrium facets in crystals are due to the presence of cusps[8,9] in the surface energy density $\gamma(\hat{\mathbf{n}})$ in the angular space, $\hat{\mathbf{n}}$ being the unit normal to the crystal plane. The surface energy associated with a surface Σ (normal to $\hat{\mathbf{n}}$) which is macroscopically flat but can have variations on atomic scales is

$$F_s[\Sigma] = \int d^3r_> d^3r_< \rho(\mathbf{r}_>)\rho(\mathbf{r}_<)J(\mathbf{r}_> - \mathbf{r}_<)$$
$$= \int d^3A\, J(\mathbf{A})\int_{\Omega(\mathbf{A},\Sigma)} d^3r\, v(\mathbf{r},\mathbf{A}),$$

where $\mathbf{r}_>,\mathbf{r}_<$ are on different sides of Σ, $2J(\mathbf{A})$ is the interaction between two atoms separated by $\mathbf{A}$, and $\Omega(\mathbf{A},\Sigma)$ is the volume swept through by Σ when it is translated along $-\mathbf{A}$. Equation (1) implies $F_s[\Sigma] = \sum_\tau \times J(\mathbf{A}_\tau)\int_{\Omega(\mathbf{A}_\tau,\Sigma)} d^3r\, h(\mathbf{r},\mathbf{A}_\tau)$ which is

$$F_s[\Sigma] = \sum_\tau J(\mathbf{A}_\tau)\langle h(\mathbf{r},\mathbf{A}_\tau)\rangle_{\Omega(\mathbf{A}_\tau,\Sigma)}\int_{\Omega(\mathbf{A}_\tau,\Sigma)} d^3r. \tag{2}$$

For systems where the average density of bonds over the surface is identical to that in the bulk, i.e.,

$$\langle h(\mathbf{r},\mathbf{A})\rangle_{\Omega(\mathbf{A},\Sigma)} = h(\mathbf{A}), \tag{3}$$

Eq. (2) then implies a surface energy density [with use of the fact that

$$\int_{\Omega(\mathbf{A},\Sigma)} d^3r = \int_\Sigma dS(\mathbf{r})\,|\hat{\mathbf{n}}(\mathbf{r})\cdot\mathbf{A}| = |\hat{\mathbf{n}}\cdot\mathbf{A}|\,(\text{area})],$$

$\gamma(\hat{\mathbf{n}}) = \sum_\tau |\hat{\mathbf{n}}\cdot\mathbf{A}_\tau|g(\hat{\mathbf{A}}_\tau)$, where $g(\hat{\mathbf{A}}_\tau) = \sum_{|\mathbf{A}_\tau|} J(\mathbf{A}_\tau) \times h(\mathbf{A}_\tau)|\mathbf{A}_\tau|$. If the system has a point-group symme-

try, the unit vectors $\hat{\mathbf{A}}_\tau$ can be grouped into disjoint sets such that vectors in the same set transform among themselves under the group operations. By symmetry, the energies $g(\hat{\mathbf{A}}_\tau)$ must be the same within each set, and $\gamma(\hat{\mathbf{n}})$ becomes

$$\gamma(\hat{\mathbf{n}}) = \sum_\mu g^{(\mu)} \sum_\alpha |\hat{\mathbf{A}}_\alpha^{(\mu)} \cdot \hat{\mathbf{n}}|, \tag{4}$$

where μ labels the different sets. In particular, if one assumes only nearest-neighbor interactions between atoms, there is only one such set in Eq. (4) and $\gamma(\hat{\mathbf{n}})$ reduces to the simple form

$$\gamma(\hat{\mathbf{n}}) = g \sum_\alpha |\hat{\mathbf{A}}_\alpha \cdot \hat{\mathbf{n}}|. \tag{5}$$

Surface energies of the form of Eq. (4) are known to have cusps[8,9] and will lead to equilibrium facets. For crystals with a simple basis, it is well known[9] that surface energies are the form of Eq. (5). However, Eq. (4) is a consequence of Eq. (3), which does not necessarily imply LRPO. A bond-oriented glass satisfying Eq. (3), referred to as a simple bond-oriented glass (SBOG), will have facets.

It should be noted that Eq. (3) is sufficient but not necessary for faceting. Since $\mathbf{A}$ is of atomic size, for some systems the volume $\Omega(\mathbf{A},\Sigma)$ may not be big enough for the average $\langle h(\mathbf{r},\mathbf{A}) \rangle_{\Omega(\mathbf{A},\Sigma)}$ to reach the bulk value. However, PBOS's that do not satisfy Eq. (3) can still have facets. The surface energy of these systems will depend on the average normal $\hat{\mathbf{n}}$, as well as on the location and the shape of the surface Σ, i.e., $\gamma = \gamma(\hat{\mathbf{n}},\Sigma)$. The surface energy $\gamma(\hat{\mathbf{n}})$ determining the equilibrium shape is obtained by minimization of $\gamma(\hat{\mathbf{n}},\Sigma)$ within the family of surfaces Σ with specified average orientation $\hat{\mathbf{n}}$. As shown in the next section, perfect quasicrystals (QC's) and quasiglasses (QG's) are such systems.

(2) *Surface energy for QC's and QG's with arbitrary symmetry.*—The QC's that we consider are 3D Penrose lattices generated by the generalized dual method (GDM)[10] with atoms placed at the vertices of the tiles. In the GDM, one considers N sets of equally spaced planes $\{P_n: \mathbf{r} \cdot \mathbf{k}_n = I_n\}$ normal to N vectors $\mathbf{k}_n$ in a "dual" space (I_n are integers, $n = 1$ to N). The planes P_n partition the dual space into polyhedral regions, each labeled by a set of N integers $J_n = [\mathbf{r} \cdot \mathbf{k}_n]$, where $[x]$ is the integral part of x and $\mathbf{r}$ is any point in the polyhedral region. The real-space quasilattice is given by $\sum_n J_n \mathbf{a}_n$, where the $\mathbf{a}_n$ are the nearest-neighbor bonds in the bulk and satisfy $\sum_n k_n^i a_n^j = \delta^{ij}$. As shown in the Appendix, the surface energy density of this QC is

$$\gamma(\hat{\mathbf{n}}) = J \sum_{n > m} |\hat{\mathbf{n}} \cdot \mathbf{k}_n \times \mathbf{k}_m|. \tag{6}$$

If $\mathbf{k}_n$ and hence $\mathbf{a}_n$ are the vertex vectors of an icosahedron, Eq. (6) says that even if the bonds in the bulk are all along $\langle \mathbf{a}_n \rangle$, the vectors $\mathbf{A}_\alpha$ in Eq. (5) are of the form $\mathbf{a}_n \times \mathbf{a}_m$, which are the edge vectors of an icosahedron. The origin of this difference can be traced back to the fact that Eq. (3) is violated in this case (a fact that is straightforward to verify by use of the GDM).

The applicability of Eq. (6) extends beyond the QC structures. As shown in the Appendix, even when the planes P_n in dual space are randomly instead of equally spaced, with the effect of randomly flipping a large number of tiles in a perfect QC, the surface energies of the resulting structures (QG's) are still given by Eq. (6). The structures of a 2D QG and the corresponding QC are depicted in Fig. 1. Numerical calculations of the diffraction pattern of 2D QG's of different randomness (for sizes up to 76000 tiles) show that their diffraction peaks all have widths (unrelated to finite-size effects) reflecting the loss in positional order.

While the surface energies of QG's have cusps, the surfaces $z_0(\mathbf{r})$ for the $T = 0$ facets have a height-difference correlation function $w(\mathbf{r}) = \langle [z_0(\mathbf{r}+\mathbf{s}) - z_0(\mathbf{s})]^2 \rangle_{\text{sa}} \sim r$ in both 2D and 3D, where $\langle \ldots \rangle_{\text{sa}}$ indicates a spatial average over the surface. This random-
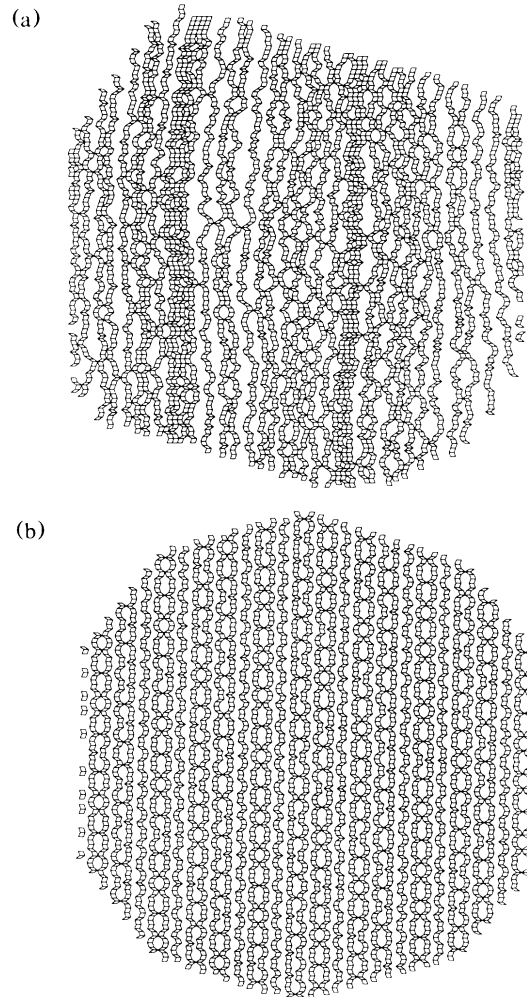
(a)

(b)

FIG. 1. (a) QG with 4.1×10^3 tiles and randomness $\Delta/D = 0.9$, D being the mean spacing between parallel dual-space lines, and Δ the spacing fluctuation. Only tiles generated by one set of dual lines are shown. (b) Corresponding QC. The flat surfaces are computer cuts, not facets.

walk result can be shown both numerically and analytically. Now, surfaces with thermal average $g(\mathbf{r}) = \langle [h(\mathbf{r}+\mathbf{s}) - h(\mathbf{s})]^2 \rangle \sim r$ in 2D or $\ln r$ in 3D, as $r \to \infty$, are conventionally[1] referred to as rough, where $h(\mathbf{r})$ is the fluctuation from the $T=0$ surface $z_0(\mathbf{r})$. The resolution to the apparent contradiction between cusps in $\gamma(\hat{\mathbf{n}})$ (producing facets and implying positive step energies) and the behavior of $w(\mathbf{r})$ lies in the distinction between $w(\mathbf{r})$ and $g(\mathbf{r})$. Indeed, $g(\mathbf{r})$ measures thermal fluctuations, and it is at the thermal roughening temperature T_R, where $g(\mathbf{r})$ first diverges as $r \to \infty$, that the step energy vanishes (the associated facet shrinking to zero size[1]) and the surface *loses its rigidity* with respect to changes in orientation. Because the $T=0$ step energy is positive, we expect $T_R > 0$ in 3D. In contrast, the behavior $w(\mathbf{r}) \sim r$ has *no connection to orientational rigidity,* merely reflecting the underlying system geometry.[11] Further, the $T=0$ surface is flat in the sense that $[w(\mathbf{r})]^{1/2}/r \to 0$ as $r \to \infty$.

(3) *Equilibrium and growth shapes.* — The equilibrium shapes generated by the energies of Eqs. (5) and (6) can be determined by the well-known Wulff construction.[8]

(a) SBOG's: The equilibrium shapes of Eq. (5) with the bonds $\hat{\mathbf{A}}_\tau$ along the fivefold, twofold, and threefold axes of an icosahedron are shown in Figs. 2(a), 2(b), and 2(c), respectively. Figure 2(a) is a triacontahedron. Figure 2(b) is a great rhombicosidodecahedron.[12] Figure 2(c) is a polyhedron with 90 rhombic faces which come in two different sizes.

(b) Perfect QC's and QG's: If the $\mathbf{k}_n$'s in Eq. (6) are along the fivefold axes of an icosahedron, $\mathbf{k}_n \times \mathbf{k}_m$ are along the twofold axes, and the equilibrium shape is a great rhombicosidodecahedron [Fig. 2(b)]. However, if the $\mathbf{k}_n$'s are along the twofold axes, Eq. (6) takes the form $\gamma(\hat{\mathbf{n}}) = Jk^2 \sum_{\mu=1}^2 g^{(\mu)} \sum_\tau |\hat{\mathbf{n}} \cdot \hat{\mathbf{A}}_\tau^{(\mu)}|$, where $\mu = 1$, 2, and 3 represents the set of vectors parallel to the fivefold, twofold, and threefold axes of the icosahedron, and $g^{(1)} = 5(\sin \pi/5 + \sin 2\pi/5)$, $g^{(2)} = 1$, $g^{(3)} = 3 \sin \pi/3$. The resulting equilibrium shape is shown in Fig. 2(d). It has big twofold facets resembling those of a triacontahedron. If the $\mathbf{k}_n$'s are along the threefold axes, Eq. (6) takes the form $\gamma(\hat{\mathbf{n}}) = Jk^2 \sum_{\mu=1}^2 g^{(\mu)} \sum_\tau |\hat{\mathbf{n}} \cdot \hat{\mathbf{A}}_\tau^{(\mu)}|$, where the $\hat{\mathbf{A}}_\tau^{(1)}$ are along the twofold axes of an icosahedron, $\{\hat{\mathbf{A}}_\tau^{(2)}\}$ is a set of 60 vectors which align with neither the fivefold nor threefold axes, and $g^{(1)} = \frac{2}{3}$, $g^{(2)} = \sqrt{8}/3$. The equilibrium shape is a complicated polyhedron shown in Fig. 2(e)

with the large threefold facets.

It can be shown from the Wulff construction and a generalization of an observation of Herring[9] that the *equilibrium* shape generated by a surface energy of the form of Eqs. (5) or (6) can never be an icosahedron or a dodecahedron. However, in growth processes, these shapes can be realized. This is because both inverse growth rates[2] and roughening temperatures[1] are proportional to equilibrium facet sizes. Both roughening and growth tend to eliminate smaller equilibrium facets. In the case of a great rhombicosidodecahedron [Fig. 2(b)] eliminating the twofold and threefold facets will turn it into a dodecahedron. For the equilibrium shape depicted in Fig. 2(d), expanding the largest facets at the expense of all smaller ones will turn it into a triacontahedron. A similar scenario applying to the shape in Fig. 2(e) will turn it into a icosahedron.

The exact nature of the icosahedral phases remains to be settled. Among the proposed models that have claimed compatibility with the diffraction pattern and the x-ray measurements are quasicrystals with frozen-in disorder[13] and the random-packing model of Stephens and Goldman[14] (a special kind of bond-oriented glass). Both models call for positional disorder. As the particular packing scheme of Ref. 14 produces long cracks in the bulk, it is relatively unlikely in a slow growth process, where the bulk has more time to equilibrate. On the other hand, it is entirely conceivable that other random-packing schemes may produce a positionally disordered PBOS which is free of such long cracks. Among the systems we have considered, both SBOG's with bonds along fivefold axes [Fig. 2(a)] and QG's with bonds along twofold axes [Fig. 2(d)] can lead to a triacontahedral growth shape. It is suggestive that Al_6LiCu_3 can be described by such structures. Likewise, the dodecahedral grain shape[6] in Al-Mn-Si can be explained by the growth of an SBOG with bonds along twofold axes, or that of a QG with bonds along fivefold axes.

Final remarks. — We have shown that facet formation can occur in systems possessing long-range bond-orientational order but lacking LRPO. Systems with bond-orientational order can have the following weaker version of positional order which seems essential for faceting: The system is anisotropic and its atoms are organized into parallel (on the average) planes separated by a minimum distance and which can be connected by
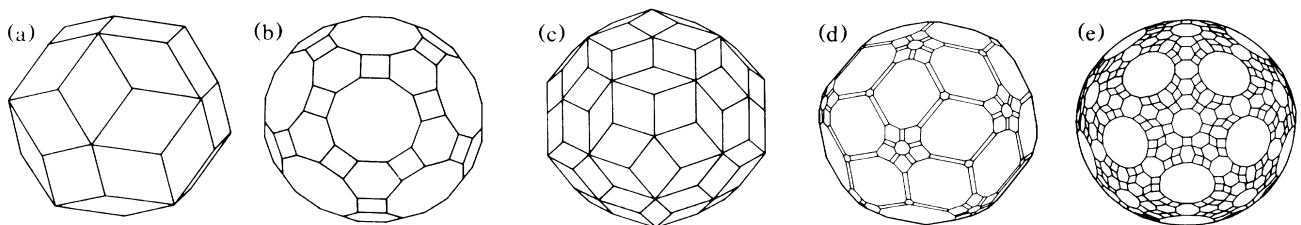

FIG. 2. The simplest equilibrium shapes of icosahedral PBOS's. See section (3) of text for details.

steps with positive energies. The precise locations of these planes or the atoms in them is apparently unimportant.

Appendix: Derivation of $\gamma(\hat{n})$ *for QC's and QG's.* — We first consider 3D perfect QC's with atoms placed at the vertices of the tiles. The atoms interact with neighbors connected by $\{\mathbf{a}_n\}$. In this derivation we show that among the macroscopically flat surfaces with an average normal $\hat{n}$, the one with the lowest energy is a surface $\Sigma(\hat{n})$ puckering up and down on a microscopic scale about a plane normal to $\hat{n}$. The surface energy of $\Sigma(\hat{n})$ is proportional to the density of polygonal vertices $\eta_d(\hat{n})$ on a plane $P_d(\hat{n})$ normal to $\hat{n}$ in dual space. These vertices are produced by the intersections between the different sets of planes P_n and $P_d(\hat{n})$, and $\eta_d(\hat{n})$ $=\sum_{n>m} |\hat{n}\cdot\mathbf{k}_n\times\mathbf{k}_m|$. These conclusions follow from the following observations: (i) Any surface Σ in real space has an image Σ_d in dual space, which is made up of polygonal surfaces corresponding to the bonds cut in real space. *The number of bonds cut by* Σ *is equal to the number of polygons F on* Σ_d. (ii) The number of polygonal vertices V on Σ_d is half the number of polygonal edges E, $E=2V$. Euler's theorem $(F+V-E=2)$ then implies that $F=V$, since both V and F are macroscopic. *The number of cut bonds of* Σ *is the same as the number of vertices on* Σ_d. (iii) The surfaces Σ_d with the lowest density of polygonal vertices are the planes P_n. Surfaces $\Sigma_d(\hat{n})$ with the lowest density of V and an average normal $\hat{n}$ can be constructed by the piecing together of segments of different planes P_n. In other words, $\Sigma_d(\hat{n})$ is a surface puckering up and down about the plane $P_d(\hat{n})$ normal to $\hat{n}$. It is easy to see that both $\Sigma_d(\hat{n})$ and $P(\hat{n})$ have the same V, and the density of V on $\Sigma_d(\hat{n})$ (per unit projected area) is

$$\eta_d(\hat{n})=\sum_{n>m}\eta(\hat{n})_{n,m}\equiv\sum_{n>m}|\hat{n}\cdot\mathbf{k}_n\times\mathbf{k}_m|.$$

(iv) The real-space image $\Sigma(\hat{n})$ of $\Sigma_d(\hat{n})$ is a surface made up of the faces of tiles. The total oriented area of $\Sigma(\hat{n})$ associated with a large projected area S_d of $\Sigma_d(\hat{n})$ (or area in P_n) is

$$S(\hat{n})=\sum_{n>m}\mathbf{a}_n\times\mathbf{a}_m\eta(\hat{n})_{n,m}S_d\,\text{sgn}(\hat{n}\cdot\mathbf{k}_n\times\mathbf{k}_m)=\hat{n}S_d,$$

with use of the relation $\sum_n \mathbf{k}_n^i \mathbf{a}_n^j=\delta^{ij}$. Thus, $\Sigma(\hat{n})$ is also a surface puckering about a plane normal to $\hat{n}$, *and the length scales of the real space and the dual space are identical.* This implies that the density of cut bonds per unit (projected) area of $\Sigma(\hat{n})$ is identical to $\eta_d(\hat{n})$, and hence Eq. (6). Similar calculation shows that $\gamma(\hat{n})$ $=J\sum_n|\hat{n}\times\mathbf{k}_n|$ in 2D.

It is important to note that the number of intersections of the planes P_n with $P_d(\hat{n})$ and hence the number of polygonal vertices on $P_d(\hat{n})$ *is unaffected by the change in spacing between the planes* P_n. The relation between the length scales in the real and dual spaces in this case is $S(\hat{n})=S_d\hat{n}+O(\sqrt{S_d})$. This correction to the length scale does not alter the number of cut bonds per unit

area. Hence the real-space structure generated by N sets of randomly spaced planes P_n (i.e., a QG) will have the same surface energy as a perfect QC. Similar calculation shows that the surface energy of QC's with bonds normal to the tile faces is also given by Eq. (6).

[1]See C. Rottman and M. Wortis, Phys. Rep. **103**, 59 (1984), for a general review of equilibrium crystal shapes.

[2]See A. A. Chernov, Usp. Fiz. Nauk **73**, 277 (1961) [Sov. Phys. Usp. **4**, 116 (1961)], for a review on crystal growth.

[3]B. Dubost, J.-M. Lang, M. Tanaka, P. Sainfort, and M. Audier, Nature (London) **324**, 48 (1986).

[4]F. W. Gayle, J. Mater. Res. **2**, 1 (1987).

[5]P. M. Horn, P. A. Heiney, P. A. Bancel, F. W. Gayle, L. J. Jordon, S. LaPlaca, and J. Angilello, to be published; P. A. Heiney, P. A. Bancel, P. M. Horn, and F. W. Gayle, to be published.

[6]J. L. Robertson, M. E. Misenheimer, S. C. Moss, and L. A. Bendersky, Acta. Metall. **34**, 2177 (1986).

[7]This is because, in general, the larger the $T=0$ facet, the larger its step energy, and the slower its growth velocity. The anisotropy of its growth velocity $\mathbf{v}(\hat{n})$ implies that the largest facets of the stationary growth shape $\mathbf{r}_0(\hat{n})$ are also the largest $T=0$ facets (see Ref. 2).

[8]G. Wulff, Z. Kristallogr. **34**, 449 (1901).

[9]C. Herring, Phys. Rev. **82**, 87 (1951).

[10]The following version of the GDM with $\sum_n \mathbf{k}_n^i \mathbf{a}_n^j=\delta^{ij}$ is a slight modification of that of J. E. S. Socolar, P. J. Steinhardt, and D. Levine, Phys. Rev. B **32**, 5547 (1985), where $\mathbf{k}_n=\mathbf{a}_n$, and can be shown to be equivalent to the projection method. See S. Gahler and J. Ryner, J. Phys. A **19**, 267 (1986), and T. L. Ho, to be published.

[11]To illustrate that $w(\mathbf{r})$ is unrelated to cusps in $\gamma(\hat{n})$, consider a 3D cubic lattice with atoms placed at the vertices. By shearing neighboring columns of cubes such that the vertical bonds remain fixed in direction and length, one can deform the original lattice planes normal to $\hat{z}$ to different types of random surfaces $z_0(\mathbf{r})$ with $w(\mathbf{r})\sim r^\beta$, $\beta<2$, while keeping the mean orientation $\hat{z}$ invariant. The following are obvious: (a) The fluctuating surface $z_0(\mathbf{r})$ is still the minimum energy surface. (b) The bulk contains a sequence of equivalent surfaces $z_0(\mathbf{r})$ separated from each other by vertical bonds. (c) The step energy and thermal roughening of this surface are determined by the vertical bonds, and are the same as for the perfect cubic lattice. (d) The surface energy of the two systems differs by a trivial geometric factor.

[12]A. Garg and D. Levine, to be published.

[13]P. M. Horn, W. Malzfeldt, D. P. DiVincenzo, J. Toner, and R. Gambino, Phys. Rev. Lett. **57**, 1444 (1986).

[14]P. W. Stephens and A. I. Goldman, Phys. Rev. Lett. **56**, 1168 (1986).